

Halogen Bonds: Benchmarks and Theoretical Analysis

Sebastian Kozuch^{*,†,§} and Jan M. L. Martin^{†,‡}

[†]Department of Organic Chemistry, Weizmann Institute of Science, IL-76100 Rehovot, Israel

[‡]Center for Advanced Scientific Computing and Modeling (CASCAM), Department of Chemistry, University of North Texas, Denton, Texas 76203, United States

Supporting Information

ABSTRACT: We carried out an extensive survey of wave function and DFT methods to test their accuracy on geometries and dissociation energies of halogen bonds (XB). For that purpose, we built two benchmark sets (XB18 and XB51). Between the DFT methods, it was found that functionals with high exact exchange or long-range corrections were suitable for these dimers, especially M06-2X, ω B97XD, and double hybrids. Dispersion corrections tend to be detrimental, in spite of the fact that XB is considered a noncovalent interaction. Wave function techniques require heavy correlated methods (i.e., CCSD(T)) or parametrized ones (SCS-MP2 or SCS(MI)MP2). Heavy basis sets are needed to obtain high accuracy, such as aVQZ or aVTZ+CP, and ideally a CBS extrapolation. Relativistic ECPs are also important, even for the bromine based dimers. In addition, we explored some XB with new theoretical tools, the NCI (“Non-Covalent Interactions”) method and the NOFF (“Natural Orbital Fukui Functions”).



INTRODUCTION

Halogen bonds^{1–7} (“XB” for short) are ubiquitous in biochemistry^{8,9} and materials chemistry.^{10,11} In other branches of chemistry, they are less prominent, probably due to the fact that the bond’s energy is comparable to, and usually smaller than, the entropy loss in dimer formation,^{12,13} not to mention the significant charge stabilization by the solvent when dealing with charged species.^{13–15} However, the utility of halogen bonds has been harnessed for some specific reactions in solvent,^{16–24} where strong XB interactions are involved, or multidentate species can overcome the entropic obstacle, much like the chelate effect.

The halogen bond is characterized by the halogen acting as a Lewis acid (electron acceptor, or “halogen donor” in this context), thus attracting Lewis bases. This effect can naively be considered opposite to the nature of a normally negatively charged halide. However, the electron density distribution creates a positive spot *trans* to the accompanying atom (the “ σ hole”). Because of this, the XB is strongly dependent on the R–X…B angle (with “B” being the Lewis base), which exhibits a potential minimum at 180°, thus imposing a linear geometry.^{3,25–29}

The stronger halogen bonds involve more electropositive halogens, that is, iodine will make more stable dimers than bromine, and bromine in turn more than chlorine (fluorine was supposed to be inert as a halogen donor, but recent studies have found that there are exceptions^{30–32}). Also, the stronger the inductive effect of the R group, the stronger the XB. This trend follows Hammett’s σ constant,³³ but some exceptions do exist,³⁴ showing that XBs can be more complex than a simple

linear rule. It must be noted that, similar to the halogen bond, recently the chalcogen and pnictogen bonds (based on elements of group 16 and 15) have also been “rediscovered.”^{35–38}

A number of groups analyzed the XB trying to explain the forces that make it happen. To this end, several energy decomposition analyses were used (SAPT,^{39,40} IMPT,⁴¹ EDA,^{42,43} and others^{44,45}), sometimes reaching differing conclusions on the importance of each component (electrostatic, dispersion, polarization, and charge transfer to the σ^* LUMO orbital of the R–X bond^{5,43,46}). One of the reasons for this dispute resides in the different weight of these components that each XB system has.³⁹ Also, diverse computational methods (DFT or ab initio, or different basis sets) and decomposition analysis may provide a full spectrum of results.

In any case, all these “bonding models” are *noumena*,^{47–49} intellectual constructs that help us rationalize the bonding patterns but do not refer to real quantum mechanical observables of the system (i.e., “*phenomena*”). This means that there is no “last word” on the results of the decomposition analysis of the XB (or any other bond), but still it can help us understand it. The *noumena* in the chemical bonding models were allegorically associated by Frenking with the mythical unicorn, an “animal whose appearance is known to everybody although nobody has ever seen one... a creature which brings law and order, health and good fortune, fame and satisfaction in an otherwise chaotic and disordered world.”⁵⁰ Halogen bonds

Received: December 4, 2012

Published: March 1, 2013



are indeed a complex mixture of several bonding components which, even if they are not totally independent quantities, are tools that can help us understand its nature. But of course, when dissecting them, great care must be taken in their interpretation, lest that instead of a unicorn we would find a siren ("dangerous and devious creatures, portrayed as *femmes fatales* who lured nearby sailors with their enchanting music and voices to shipwreck on the rocky coast of their island"⁵¹).

A good theoretical method for the estimation of geometries and energies of XB must properly cover all its bonding components (electrostatic, dispersion, polarization, and charge transfer), trying not to rely on error compensation.⁴⁸ In this work, we start with a discussion of some tools for the analysis of XB. Then, we study the accuracy of several wave function and DFT methods on the geometry and dissociation energy of halogen bonds with different strengths and characteristics. This can be used as a guidance for quantum mechanical studies of real systems, or to provide geometries and energies for accurate force fields.⁵² For the geometries, a small set of 18 small dimers was considered ("XB18"), while for the energies, a larger set of 51 dimers ("XB51") with a broad range of association energies was used. In addition, we considered the accuracy of different basis sets, the amount of exact exchange in hybrid functionals, the importance of relativity effects, and the necessity of dispersion corrections. Some previous benchmarks and accuracy studies have been carried out on XB, based on experimental⁵³ or theoretical³¹ data; the recent work of Řezáč et al stands out among them,⁵⁴ providing a benchmark (named "X40") of halogenated molecules with and without XB.

THEORETICAL METHOD

The importance of dynamical correlation for noncovalent interactions (NCI) depends on the balance between electrostatics and dispersion: it can range from about 30% of the interaction energy for a water dimer⁵⁵ to 100% or more for purely dispersive interactions such as in noble gas dimers (where the SCF component is typically repulsive). As such, dynamical correlation needs to be treated properly with adequately post-HF corrections and basis sets.^{7,44} For the XB18 set, we calculated the benchmark dissociation energies at the CCSD(T)/CBS level, extrapolating to the complete basis set from the aug-cc-pVQZ basis sets, with X = Q and S,^{56–58} and the Br and I using the ECP version of them, commonly called aug-cc-pVQZ-PP (unless specified, we will simply call this basis "aVQZ").^{59,60} For the extrapolation procedure, we employed eq 1 (being $L = S$), with $\alpha = 5$ for the SCF energy and the CCSD triplet coupled pairs and $\alpha = 3$ for the singlets and the (T) connected triples.

$$E_{\text{CBS}}^{\text{CCSD(T)}} = E_L + \frac{E_L - E_{L-1}}{(L/L - 1)^\alpha - 1} \quad (1)$$

In the search for a computationally (both in CPU time and in other resource demands, such as RAM and I/O) more lightweight procedure for the much larger XB51 set, we compared $E_{\text{CBS}}^{\text{CCSD(T)}}$ of eq 1 with the MP2-based extrapolation:

$$E_{\text{CBS}(\text{MP2})}^{\text{CCSD(T)}} = E_{\text{aVQZ}}^{\text{CCSD(T)}} - E_{\text{aVQZ}}^{\text{MP2}} + E_{\text{CBS}}^{\text{MP2}} \quad (2)$$

where $E_{\text{CBS}}^{\text{MP2}}$ was estimated using the same formula as $E_{\text{CBS}}^{\text{CCSD(T)}}$ (eq 1), but using density fitting (a.k.a. resolution of the identity) in the MP2 steps, as well as "only" aVQZ-aVQZ basis sets. This lighter method proved to yield results virtually

identical to the more rigorous CCSD(T)/CBS extrapolation for the XB18 set (see Table 4).

The geometry optimization of XB18 was done at the CCSD(T)/aVQZ level, again with the aVQZ-PP basis set on Br and I. For the XB51, the geometries were calculated at the aB97X/aVTZ level. All the wave function-based results were calculated with MOLPRO 2010,^{61,62} while the DFT calculations were carried out with Gaussian 09, revision C.1,⁶³ of which an in-house modification was employed for the DSD-PBEP-B95 energies and the D2-including geometry optimizations. Additional D2 and D3 dispersion corrections were calculated with the DFT-D3 program.⁶⁴

The noncovalent interaction regions were calculated with NCI Plot^{65–67} from the aB97X/6-311g** electronic density and graphed with VMD.⁶⁸

RESULTS AND DISCUSSION I: SOME TOOLS FOR THE ANALYSIS OF HALOGEN BONDS

NCI Plot. The strength of the XB depends mostly on the electrophilicity of the Lewis acid (the "halogen donor") and the nucleophilicity of the Lewis base (the "halogen acceptor"). An elegant way to assess the characteristics of the XB is by analyzing the sign of λ_2 , the second derivative of the electronic density in the perpendicular direction of the bond ($\partial^2\rho/\partial y^2$), in a critical point where the reduced gradient

$$s = \frac{1}{2(3\pi^2)^{1/3}} \frac{|\nabla\rho|}{\rho^{4/3}} \quad (3)$$

is equal to zero. A negative λ_2 is a sign of attractive interaction (with an accumulation of density perpendicular to the bond), while a positive value implies steric repulsion (density depletion). Van der Waals interactions are described by low electron density (ρ) at the critical points, and thus $\text{sign}(\lambda_2)\cdot\rho \lesssim 0$. This method, called NCI (for noncovalent interactions), was designed by Yang's group.^{66,67} At the time of writing this manuscript, a first application of the method for halogen bonds was reported by Pinter et al.⁴⁵

In Figure 1, two model halogen bonded systems of different strengths are shown, with the graph of the reduced gradient vs $\text{sign}(\lambda_2)\cdot\rho$. The FI···NCH dimer, with a very electrophilic

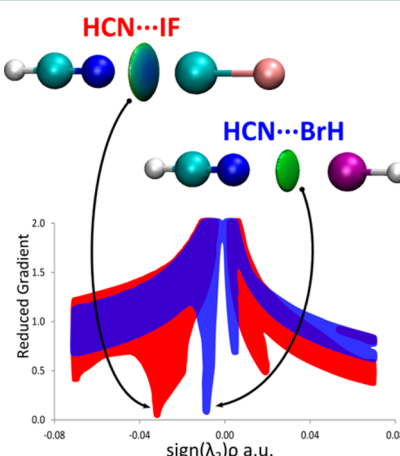


Figure 1. Two halogen bonds of different strengths (depicted by an interaction surface around the critical point) and the graph of the reduced electron density gradient vs $\text{sign}(\lambda_2)\cdot\rho$, rendered using NCI Plot.⁶⁵ The more stable FI···NCH dimer has a lower λ_2 than HBr···NCH.

halide, has a fairly strong XB of 9.45 kcal/mol, while the HBr···NCH is barely stable, with a dissociation energy of 1.41 kcal/mol. The former compound has a ρ value well in the range of typical hydrogen bond systems ($\rho \approx 0.03$ au), showing more electrostatic attraction, whereas the latter shows characteristics of a more dispersive interaction ($\rho \approx 0.01$ au).³⁹

The σ -hole is surrounded by a negative ring composed of the halogen's p_x and p_y atomic orbitals. In an opposite trend compared to the XB, this negative ring has some nucleophilic power and can provide an extra stabilization on the dimer.^{69–72} This amphoteric feature of the halogen atom can mask the lower bonding energy of a pure XB. Moreover, the weaker the XB, the stronger the basicity of the negative ring on the halogen atom.

For instance, in the XB18 set we considered two halogen acceptors: hydrogen cyanide and formaldehyde. The first generates linear geometries which are attached by pure halogen bonds (see Figure 1). H₂CO, however, has acidic hydrogen atoms that can form weak hydrogen bonds with the negative ring of the halogen. In Figure 2, the NCI Plot shows that the

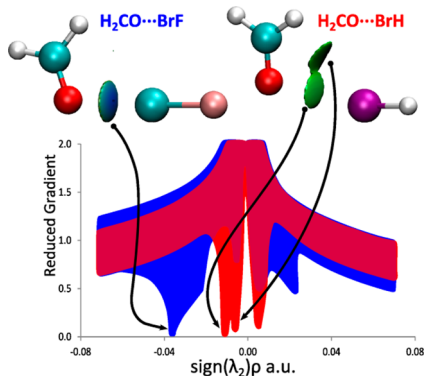


Figure 2. NCI Plot. The stronger halogen donor FBr generates only one interaction with formaldehyde (the halogen bond), with one low $\text{sign}(\lambda_2)\rho$ at the critical point. Hydrogen bromide forms a weaker XB with higher $\text{sign}(\lambda_2)\rho$, but a hydrogen bond is simultaneously formed due to the higher electronic density on the negative ring of the halide.

FBr Lewis acid can form a strong XB with $\rho \approx 0.04$, while the weaker acidic halogen in HBr has a $\rho \approx 0.01$. However, a second interaction surface with similar ρ appears at the interface between the bromine and the hydrogen, depicting the weak H-bond. When comparing the dissociation energies of both halogen donors with H₂CO and HCN, we can see that FBr bonds similarly with the two halogen acceptors (8.60 kcal/mol for FBr···OCH₂ and 7.61 kcal/mol for FBr···NCH), but HBr has a 50% stronger bond when the hydrogen bond is added (2.10 kcal/mol for HBr···OCH₂, 1.41 kcal/mol for HBr···NCH). As a result, also the geometry is affected to favor the two interactions (see the Supporting Information for the geometries).

Fukui Function. Another way to rationalize the double interaction of weak halogen donors is by looking at the Fukui function^{45,73,74} of both the halide species and the formaldehyde. This function shows the distribution of an infinitesimal charge added or removed from a molecule, according to

$$f^+(\mathbf{r}) = \left(\frac{\partial \rho(r)}{\partial N} \right)^+ = \rho_{N+1}(\mathbf{r}) - \rho_N(\mathbf{r}) \quad (4a)$$

$$f^-(\mathbf{r}) = \left(\frac{\partial \rho(r)}{\partial N} \right)^- = \rho_N(\mathbf{r}) - \rho_{N-1}(\mathbf{r}) \quad (4b)$$

An added negative charge will tend to go to the places of high f^- (acid zones, susceptible to a nucleophilic attack), while a high f^+ shows the most probable places to act as an electron donor (basic zones, susceptible to an electrophilic attack). These functions do not provide information on the probability of a charge transfer but on its regioselectivity.

Figure 3 depicts the Fukui functions of a strong halogen donor (FI), a weak one (HBr), and a halogen acceptor

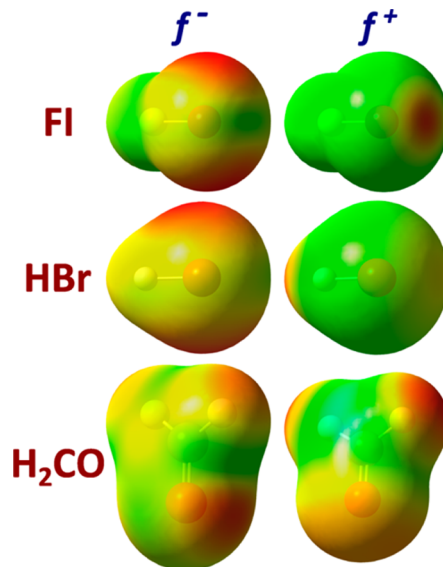


Figure 3. Fukui functions of a strong halogen donor (FI), a weak one (HBr), and a halogen acceptor (H₂CO). f^- shows the places with highest probabilities of acting as electron donors, and f^+ shows the places of electron acceptors (in red, the most active zones).^{73,74}

(H₂CO). FI clearly shows the σ -hole on the f^+ surface, suggesting the involvement of the p_z orbital of the iodine in the covalent bond. The same surface for HBr is less clear in this respect, as the active region is at the hydrogen side, indicating the less active bromine and the “desire” of the molecule to “back-flip” and form a more traditional H-bond. The f^- surface for both molecules shows that, given the possibility of acting as a Lewis base instead of an X-donor, the regioselectivity will be centered at the I and Br, directed by a p_y orbital.⁷⁵ The same surfaces on the formaldehyde show the tendency of the oxygen lone pair region to act as a nucleophile, and the hydrogens as electrophiles. A more complete study of the Fukui functions applied to halogen bonds can be found in the recent work of Pinter et al.⁴⁵

Natural Orbital Fukui Function (NOFF). A similar analysis can be made by comparing the natural orbital Fukui functions (NOFF),⁷⁶ which considers the effect of the addition or removal of charge on the natural bonding orbitals, according to

$$f_{\text{nbo}}^+ = \left(\frac{\partial n_{\text{nbo}}}{\partial N} \right)^+ = n_{\text{nbo}}^{N+1} - n_{\text{nbo}}^N \quad (5a)$$

$$f_{\text{nbo}}^- = \left(\frac{\partial n_{\text{nbo}}}{\partial N} \right)^- = n_{\text{nbo}}^N - n_{\text{nbo}}^{N-1} \quad (5b)$$

The NBOs with highest f_{nbo}^+ and f_{nbo}^- are the strongest electron acceptors and donors, respectively. In Figure 4, we

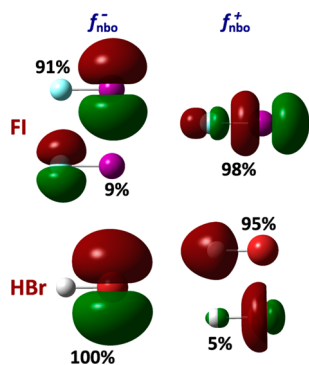


Figure 4. Highest natural orbital Fukui functions (NOFF) for the strong halogen donor FI and the weak HBr.

show these orbitals for the FI and HBr cases. According to f_{nbo}^- , the nucleophilic NBOs are the “lone pairs” on the I and Br (clearly based on the p_y orbitals), with a small basicity on the fluoride. f_{nbo}^+ shows that the electrophilic NBO for the strong halogen donor FI is the virtual σ^* antibonding orbital, which acts as the electronic acceptor; this is in accordance with all of the traditional NBO studies that describe the charge transfer to this orbital.³⁹ However, the HBr σ^* does not appear as a possible electron acceptor. As in Figure 3, the hydrogen is the atom that will be prone to nucleophilic attack, given the possibility (i.e., if the base approaches the molecule from the H side). The highest NOFF is an unoccupied “Rydberg” orbital based on an s atomic orbital. But if a nucleophile is forced to come from the Br side, then there is the possibility of accepting the extra charge into an sp Rydberg orbital, creating the conditions for a charge transfer and a weak XB.

It is possible to conclude here that weak halogen bonds can be sometimes misleading, in the sense that they can be metastable structures or artificially stabilized by other non-covalent interactions. Also, the more complex the system, the higher the possibility of having stronger bonds due to non-XB forces. This can be seen in the $\text{MeI}\cdots\text{Pd}(\text{PH}_3)_2\text{HCl}^-$ dimer (a member of the XB51 set, with a dissociation energy of 5.05 kcal/mol), where two attraction forces are added to the XB through the negative ring of the iodine, one to the phosphine and one to the Pd metal center (see the NCI Plot in Figure 5).

RESULTS AND DISCUSSION II: HALOGEN BOND GEOMETRIES

XB18 Set. This set consists of 18 dimers of typical halogen bond small systems. The simplicity of the dimers allows one to

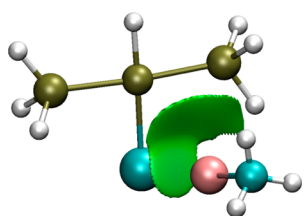


Figure 5. NCI Plot of the $\text{MeI}\cdots\text{Pd}(\text{PH}_3)_2\text{HCl}^-$ dimer, showing the interactions of the iodine with the phosphine and the palladium, further stabilizing the XB with the chloride.

perform geometry optimizations with high accuracy; thus it was used to benchmark the XB distances at the CCSD(T)/aVQZ level. The set contains all of the combination of nine diatomic halogen donors (Br_2 , BrI , ClBr , ClI , FBr , FI , HBr , HI , and I_2) with two halogen acceptors (NCH and H_2CO). With hydrogen cyanide, all the geometries are linear (see Figure 1), while the formaldehyde generates planar dimers (see Figure 2).

The resulting dissociation energies range from the very labile $\text{HBr}\cdots\text{NCH}$ (1.41 kcal/mol) to $\text{FI}\cdots\text{OCH}_2$, with a respectable XB of 10.09 kcal/mol (see Table 1). Not surprisingly, the

Table 1. Dissociation Energies and Halogen Bond Distances for the XB18 set^a

	diss. E (kcal/mol)	XB dist. (Å)
$\text{HBr}\cdots\text{NCH}$	1.41	3.236
$\text{HBr}\cdots\text{OCH}_2$	2.10	3.112
$\text{HI}\cdots\text{NCH}$	2.24	3.298
$\text{HI}\cdots\text{OCH}_2$	2.87	3.163
$\text{Br}_2\cdots\text{NCH}$	3.63	2.880
$\text{I}_2\cdots\text{NCH}$	4.03	3.029
$\text{Br}_2\cdots\text{OCH}_2$	4.42	2.739
$\text{ClBr}\cdots\text{NCH}$	4.47	2.793
$\text{I}_2\cdots\text{OCH}_2$	4.78	2.892
$\text{ClBr}\cdots\text{OCH}_2$	5.27	2.663
$\text{BrI}\cdots\text{NCH}$	5.31	2.900
$\text{BrI}\cdots\text{OCH}_2$	6.10	2.783
$\text{ClI}\cdots\text{NCH}$	6.31	2.816
$\text{ClI}\cdots\text{OCH}_2$	7.08	2.716
$\text{FBr}\cdots\text{NCH}$	7.61	2.528
$\text{FBr}\cdots\text{OCH}_2$	8.60	2.452
$\text{FI}\cdots\text{NCH}$	9.45	2.613
$\text{FI}\cdots\text{OCH}_2$	10.09	2.571

^aThe geometries were calculated at the CCSD(T)/aVQZ level and the energies at CCSD(T)/CBS.

halogen bond distance between the monomers is inversely correlated to the bond strength (see Figure 6). This distance is the measure we used to test the accuracy of different wave function and DFT methods.

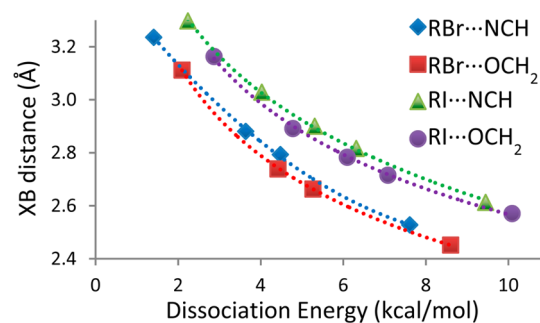


Figure 6. Halogen bond length vs dissociation energy for the XB18 set. Each series corresponds to a different electron-withdrawing atom on the Lewis acid ($\text{R} = \text{H, I, Br, Cl, F}$).

In Table 2 and Figure 7, the mean signed errors (MSE) and root-mean-square deviations (RMSD) of the XB distances are depicted, as a measure of the bias and accuracy of 42 DFT and four WF methods. At first glance, it can be said that achieving good accuracy is not simple, and although on average hybrid functionals are better than pure GGA and double hybrids are

Table 2. Mean Signed Error, Root Mean Square Deviation, and Maximum Error on the XB Distances of the XB18 Set (in Å)

	MSE	RMSD	Max	WF	LDA	GGA	Meta GGA	hybrid (%HF)	disp. corr.	double hybrid
HF	0.302	0.309	0.418	X						
MP2	-0.095	0.098	-0.153	X						
SCS-MP2	-0.024	0.031	-0.072	X						
SCS(MI)MP2	-0.039	0.043	-0.077	X						
SVWN5	-0.332	0.341	-0.462	X						
B97D ^a	0.037	0.112	0.197			X			X	
BB95	-0.038	0.157	0.426			X	X			
BLYP	-0.017	0.098	0.200			X				
BP86	-0.106	0.149	-0.241			X				
HCTH	0.130	0.192	0.359			X				
mPW91	-0.089	0.151	-0.244			X				
mPWLYP	-0.056	0.088	-0.165			X				
PBEhPBE	-0.127	0.150	-0.242			X				
PBE	-0.122	0.151	-0.257			X				
PBE-D ^b	-0.120	0.153	-0.261			X			X	
PBEK CIS	-0.075	0.115	-0.229			X	X			
TPSS	-0.098	0.156	-0.216			X	X			
TPSS-D ^b	-0.108	0.150	-0.227			X	X		X	
M06L	-0.046	0.065	-0.152			X	X			
τ HCTH	-0.028	0.167	0.337			X	X			
B1B95	0.001	0.070	0.144				X	28		
B3LYP	0.001	0.060	0.139					20		
B3LYP-D ^b	0.000	0.054	-0.099					20	X	
X3LYP	-0.016	0.049	-0.088					22		
B98	-0.009	0.059	0.110					22		
B97-1	-0.018	0.052	-0.102					21		
BHandHLYP	0.033	0.041	0.088					50		
BMK	0.002	0.022	-0.065				X	42		
M06	-0.061	0.070	-0.126				X	27		
M062X	-0.009	0.028	-0.072				X	54		
M06HF	-0.019	0.089	0.211				X	100		
mPW1PW91	-0.032	0.094	0.189					25		
PBE0	-0.061	0.087	-0.152					25		
PBE0-D ^b	-0.060	0.086	-0.159					25	X	
PBEhPBE	-0.067	0.089	-0.142					25		
TPSSh	-0.072	0.132	0.206				X	10		
TPSSh-D ^b	-0.081	0.122	-0.188				X	10	X	
CAM-B3LYP	-0.014	0.031	-0.058					var.		
LC- ω PBE	0.032	0.079	0.217					var.		
ω B97X	-0.008	0.021	-0.053					var.		
ω B97XD ^a	0.024	0.039	0.101					var.	X	
B2GP-PLYP	-0.045	0.049	-0.080						X	
B2P-LYP	-0.038	0.048	-0.086						X	
DSD-BLYP ^a	-0.048	0.053	-0.090					X	X	
DSD-PBE-P86-D2 ^a	-0.052	0.057	-0.089					X	X	
DSD-PBE-P86-noD	-0.072	0.074	-0.109						X	

^aThese functionals were parametrized including D2 dispersion correction. ^bIncluding D2 dispersion correction added on top of the functional (i.e., without reparametrizing the functional).

another step forward, from a case-by-case analysis it is difficult to generalize.

The best GGA is M06-L, while the best hybrids are BMK, M06-2X, and the long-range corrected CAM-B3LYP and ω B97X. Something in common for all these hybrid functionals is the high amount of exact exchange, a matter that we will analyze in a later section. Quite surprisingly, double hybrids were not the best choice for geometries, even though they do work well for energies (vide infra).

Wave Function Methods. The Hartree–Fock RMSD is so high that in practice the method can be considered a very

elaborate random number generator. It severely underbinds, with interaction distances too large compared to the reference. This does not come as a surprise, considering that HF lacks dynamic correlation, which is a critical stabilizing agent in noncovalent interactions.

In contrast to this, MP2 overbinds, as the “traditional” version of second order perturbation tends to overestimate dynamical correlation,⁷ SCS-MP2,⁷⁷ which scales down the same spin (c_s) and enlarges the opposite spin (c_o) components of the MP2 correction, provides one of the most accurate results on the table. Its counterpart, SCS(MI)MP2,⁷⁸ with high

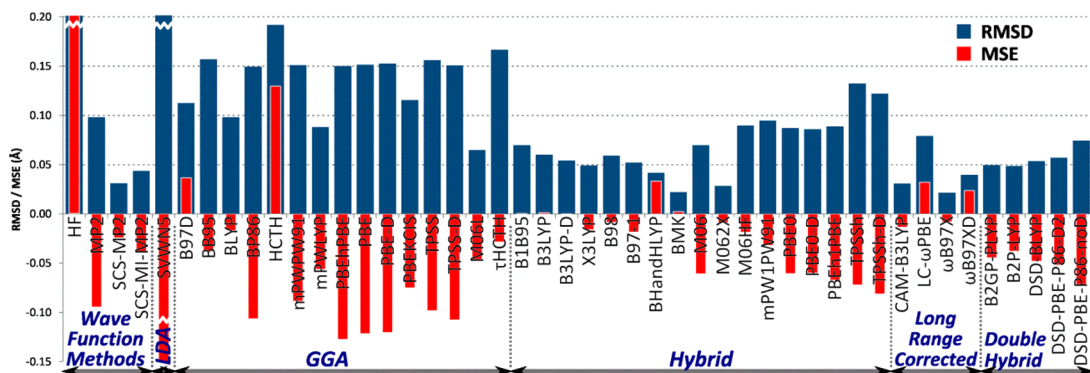


Figure 7. Root mean square deviation and mean signed error for the XB distance in the XB18 set, as the measures of accuracy and bias of different WF and DFT methods (reference: CCSD(T)/aVQZ geometries). All calculations were carried on with the aVQZ basis set.

same spin and small opposite spin MP2 correction, is also well behaved here. The question that arises is, why is SCS-MP2, known to be reliable with covalent bonds but not with noncovalent ones, as good as its “nemesis” SCS(MI)MP2, which was optimized for intermolecular interactions but fails with intramolecular ones?

The original SCS-MP2 has $c_s = 0.33$ and $c_o = 1.2$, while the MI variety has $c_s = 1.29$ and $c_o = 0.4$. The sum of coefficients for the first is 1.53 and 1.69 for the second. Both values are smaller than in the standard MP2 ($c_s + c_o = 2$), providing the rationale for the improvement. In Table 3, the RMSD of the dissociation

Table 3. RMSD of the SCS-MP2 Dissociation Energies for the XB18 Set (in kcal/mol at the CCSD(T)/aVQZ Geometry), As a Function of the Same Spin (c_s) and Opposite Spin (c_o) MP2 Components

$c_o \backslash c_s$	0	0.2	0.4	0.6	0.8	1	1.2	1.4	1.6
0	3.40	2.98	2.56	2.14	1.72	1.30	0.89	0.50	0.27
0.2	2.99	2.57	2.15	1.73	1.31	0.90	0.51	0.25	0.48
0.4	2.59	2.17	1.74	1.33	0.91	0.52	0.24	0.46	0.85
0.6	2.18	1.76	1.34	0.93	0.53	0.24	0.44	0.83	1.25
0.8	1.78	1.36	0.94	0.54	0.25	0.43	0.82	1.23	1.65
1	1.38	0.96	0.56	0.26	0.42	0.81	1.22	1.63	2.05
1.2	0.98	0.59	0.28	0.42	0.80	1.20	1.62	2.04	2.46
1.4	0.61	0.31	0.42	0.79	1.19	1.61	2.02	2.45	2.87
1.6	0.34	0.43	0.78	1.18	1.60	2.01	2.43	2.85	3.27

energies of the full set calculated at the MP2/aVQZ level are shown (geometries at CCSD(T)/aVQZ), as a function of the different spin components. As can be seen, there is a canal of accuracy around $c_s + c_o \approx 1.6$, very close to the SCS-MP2 and SCS(MI)MP2 coefficients. In other words, a scaling down of the perturbative terms, no matter which one, will correct the overbinding of MP2 in halogen bonds (which makes us wonder if this can be extrapolated to other types of interactions).

In addition to the geometric test, we checked the dissociation energies for the XB18 set with other WF methods at the CCSD(T)/aVQZ geometries, as depicted in Table 4. Again, we see that HF is quite useless and MP2, which generates bonds overly strong, is improved by both SCS-MP2 and SCS(MI)-MP2 versions. MP3 does not bring a significant improvement compared to its perturbative predecessor, with a tendency to underbind. Thus, MP2.5 brings a balance between MP2 and

Table 4. MSE and RMSD Dissociation Energies (in kcal/mol) for Wave Function Methods at the CCSD(T)/aVQZ Geometry, with Reference to CCSD(T)/CBS Energies Calculated with eq 1^a

aVQZ	MSE	RMSD	CCSD(T):	MSE	RMSD
HF	-3.15	3.29	aVDZ	0.48	0.53
MP2	0.76	0.83	aVTZ	0.08	0.16
SCS-MP2	-0.18	0.34	aVQZ	0.05	0.08
SCS(MI)MP2	0.16	0.31	aVSZ	0.02	0.04
MP3	-0.63	0.69	CCSD(T)/CBS(MP2):		
SCS-MP3	-0.53	0.62	aVDZ+MP2(TQ)	0.09	0.11
MP2.5	0.07	0.16	aVDZ+MP2(Q5)	0.02	0.04
CCSD	-0.61	0.67	aVTZ+MP2(TQ)	0.02	0.06
SCS-CCSD	-0.15	0.23	aVTZ+MP2(Q5)	-0.05	0.06
SCS(MI)CCSD	-0.02	0.12	aVQZ+MP2(Q5)	-0.04	0.05
CCSD(T)	0.05	0.08			

^aThe first columns include several methods calculated with the aVQZ basis set, while the second columns shows CCSD(T) method with different basis sets, including basis set extrapolation based on eq 2 (TQ, MP2 extrapolation based on aVTZ-aVQZ; Q5, idem with aVQZ-aV5Z).

MP3, with a remarkable accuracy. The SCS-MP3 flavor⁷⁹ (SCS-MP2 plus one-fourth of the E3 correction) is not an adequate choice for halogen bonds, as it degrades the already accurate SCS-MP2. Similar results were found by Řezáč et al. with the X40 set.⁵⁴

The accuracy of coupled-cluster with singles and doubles excitations (CCSD) is quite feeble, a sign of the strong correlation of the XB systems. Similar to MP2, a scaling of the double excitation correlation energy in the SCS-CCSD⁸⁰ and the SCS(MI)CCSD⁸¹ versions improve the accuracy of the raw CCSD, as both reparametrizations can cure the underbinding by having higher than one coefficient for both the singlet and triplet pairs.

CCSD(T) with a complete basis set approximation (eq 1) was used to obtain reference energies, so it is possible to test the convergence with the basis set and other extrapolation techniques (based on eq 2). With small basis sets, the method tends to form overly stable bonds due to basis set superposition error. This can be partially corrected by the counterpoise method (see later). The double-zeta basis set, even with diffuse functions, is far from the accuracy expected for this heavy post-HF method. However, if a basis set extrapolation is added with an MP2/CBS correction, a fast and accurate composite method is possible (especially if density fitting is used for MP2).

Although there are no big differences for the accuracy in the XB18 set when considering different basis sets for the CCSD(T) energies and the MP2 extrapolations, we found for the bigger XB51 set that using CCSD(T)/aVDZ was not as reliable as aVTZ. Therefore, we recommend as the most balanced benchmark method for bigger systems to use CCSD(T)/aVTZ + DF-MP2(QS), which was applied to the XB51 set.

Density Functional Approximations (DFA). The trends of DFT on XB geometries are far from simple. While most functionals overbind (with shorter XB distances compared to the reference), some of them are clearly underbinding. The renowned Jacob's ladder of DFT accuracy⁸² is only partially observed, with LDA at the lower rung of accuracy, pure GGA functionals considerably better, hybrid DFT usually (but not always) improving, and double hybrids coming out on top, but only on average.

Interestingly, even though dispersion corrections were designed to improve noncovalent bond interactions, in here the inclusion of the D2 method in the optimization made negligible changes. This is actually good news, considering that the bare DFAs were already overshooting the interaction energies. PBE, TPSS, B3LYP, PBE0, and TPSSh were tested with the dispersion correction, and from Table 2 and Figure 7 it can be seen that this addition was hardly noticeable. Two other functionals (B97D and ω B97XD) include such corrections, but the internal DFA parameters of them were optimized in their presence; as a result, due to the minimal effect of the D2 in these halogen bonds, B97D and ω B97XD actually underbind. ω B97X, being the sibling of ω B97XD optimized without D2, turns out to be the most accurate functional of the full set of geometries, performing even better than all the double hybrids.

The most accurate hybrid functionals have a very high exact exchange proportion (BMK, M06-2X) or a long-range corrected modulation of the exact exchange (i.e., high HF at long distance, and high DFT_X at short distance), as in CAM-B3LYP and ω B97X. In systems with charge transfer, it is not uncommon to find a requirement of high amount of exact exchange, as we will discuss later (although within limits, as can be seen from M06-HF,⁸³ which has 100% HF).

For double-hybrids, we observe rather robust behavior, with all the functionals analyzed here providing close results. However, it is slightly disappointing that, even though their accuracy is good, they are no match for the best hybrid DFT or SCS-MP2 in this XB geometric test. Nevertheless, as the double hybrids have been found to be very effective on a broad range of chemical problems,⁸⁴ they can be the choice for cases that involve bonds of a different nature, including covalent and noncovalent interactions (requiring similar computational time as any other MP2 based method).

To sum up, we recommend for geometry optimizations of systems that include halogen bonds to use ω B97X or M06-2X functionals. CAM-B3LYP and BMK are also very accurate but were designed for specific purposes (charge transfer⁸⁵ and activation energies,⁸⁶ respectively), thus they may be less “universal” than the previous ones (although M06-2X may be considered “over-fitted” to the training set and will have an erratic behavior for other systems such as with transition metals,^{87,88} not to mention their numerical stability problems⁸⁹). For larger and more time-consuming systems, the meta-GGA M06L functional is the choice, especially considering that for accurate XB calculations a large basis set is needed

(and implementations of density fitting are more widely available for “pure DFT” than for hybrid functionals).

RESULTS AND DISCUSSION III: HALOGEN BOND ENERGIES

XB51 Set. The XB51 set is much broader than the previous one, consisting of six series of 10 dimers (some of them are duplicated; thus in total there are 51 systems). Three series vary the Lewis acid, and three vary the Lewis base. We have selected these dimers to cover a wide range of elements and dissociation energies, from the almost negligible FCCH based dimers to the strongly bonded organometallic dimers with PdHP₂Cl (Figure 5),⁹⁰ including some nontraditional molecules such as lithium hydride.⁴⁰

The benchmark dissociation energies are shown in Figure 8 and Table 5 (reference energies: $E_{\text{CBS/MP2(QS)}}$, see eq 2). The

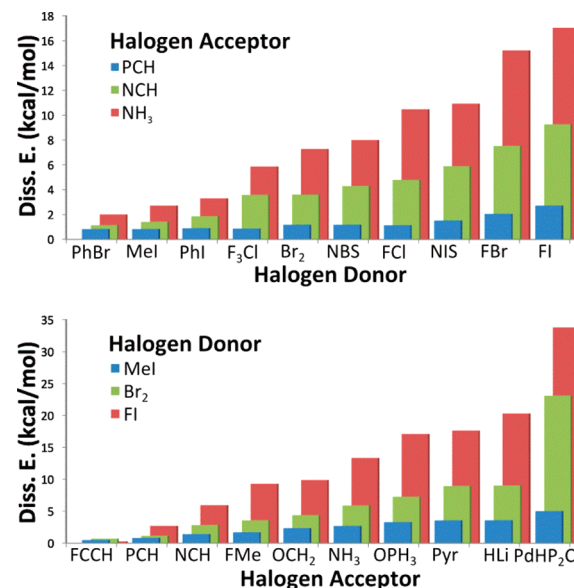


Figure 8. Graphical representation of the dissociation energies of the XB51 set, divided by the six series (three X donor and three X acceptor series).

geometries were calculated at the ω B97X/aVTZ level, one of the most accurate methods for geometry optimizations in the XB18 set (Figure 7). All the xyz geometries are included in the Supporting Information.

Table 5. Reference Dissociation Energy (in kcal/mol) for the XB51 Set, at the $E_{\text{CBS/MP2(QS)}}$ Level (see eq 2)

X donor	X acc.			X donor			
	PCH	NCH	NH3	X acc.	MeI	BrBr	
PhBr	0.85	1.15	2.02	FCCCH	0.50	0.74	0.29
MeI	0.85	1.42	2.73	PCH	0.85	1.18	2.74
PhI	0.92	1.87	3.33	NCH	1.42	2.87	5.97
F ₃ Cl	0.89	3.61	5.88	FMe	1.70	3.61	9.33
Br ₂	1.18	3.61	7.29	OCH ₂	2.39	4.41	9.94
NBS	1.19	4.32	8.02	NH ₃	2.73	5.95	13.36
FCl	1.16	4.81	10.54	OPH ₃	3.34	7.29	17.11
NIS	1.53	5.91	10.99	Pyr	3.61	9.00	17.66
FBr	2.07	7.53	15.30	HLi	3.62	9.07	20.34
FI	2.74	9.33	17.11	PdHP ₂ Cl	5.05	23.11	33.79

Relativistic Contribution. Relativistic effects can be significant in iodine chemistry due to its high weight; thus we tested if these effects also affect the halogen bonds. Quite surprisingly, relativity is important even for bromine.

To test the relativistic contribution, we compared the Douglas–Kroll (DK) Hamiltonian to the nonrelativistic one, the latter with and without relativistic ECP on the Br and Cl based dimers of the XB51 set (there are no “all electron” or DK correlation consistent basis sets for I). We used for this comparison the aVDZ basis set in the CCSD(T) calculation and extrapolated to a complete basis set according to eq 2 using df-MP2 with aVTZ and aVQZ. For the DK calculations, we used aVnZ-DK; for the nonrelativistic jobs, aVnZ; and aVnZ-PP for relativistic ECP.

Although the number of Cl based dimers is much smaller than the number of Br ones (3–18), the results are clear, as can be seen in Table 6. The ECP and all e^- are the same basis sets

Table 6. RMSD in kcal/mol for the Differences between CCSD(T) with Douglas–Kroll (DK) Hamiltonian (with aVxZ-DK Basis Set), and with Nonrelativistic Hamiltonian with Relativistic ECP (“rECP”, with aVxZ-PP) or with an All Electrons Basis Set (“all e^- ”, with aVxZ)

	rECP vs all e^-	rECP vs DK	all e^- vs DK
Br dimers	0.45	0.07	0.39
Cl dimers	0.00	0.13	0.13
all dimers	0.42	0.08	0.36

for the Cl systems, but they are slightly different from the DK one. Therefore, we see a small difference of 0.13 kcal/mol between them, even when using a CBS extrapolation (considering that relativity is small for Cl). However, for Br systems we see an RMSD of 0.4 kcal/mol when comparing relativistic to nonrelativistic methods (with only a small difference between ECP and DK methods).

Simply put, relativity must be considered for accurate halogen bond calculations, even with Br based systems. A good relativistic ECP will provide faster and better results.

Basis Set and BSSE. Like in all dissociation reactions, the basis set superposition effect (BSSE) can be severe with small basis sets.⁹¹ In halogen bonds, the mixture of dispersion, electrostatics, charge transfer, and others can affect the necessity of big basis sets. Therefore, we studied the basis set completeness for the correlation consistent family from the double to the quadruple- ζ , with or without diffuse functions and counterpoise (CP) correction. Both ω B97X and B3LYP functionals were tested, taking as a reference their aVQZ+CP values for each functional. The results are shown in Figure 9.

From the RMSD values, it can be seen that both CP correction and diffuse functions have a positive impact on the accuracy, as expected for these long-range interactions. From the MSE, we can see that the inclusion of the counterpoise method almost cancels any bias that basis set incompleteness may bring, such that the relatively small VTZ+CP has a virtually null signed error. However, from an “unsigned” (RMSD) point of view, it is clear that using the augmented version of the triple- ζ provides better results. The negligible difference between aVQZ+CP and aVQZ shows that at this level we are almost at the complete basis set limit (at least for hybrid DFT); the same cannot be said for the VQZ, evidencing the importance of the diffuse functions. These are the same trends that can be observed with H-bonds.⁵⁵

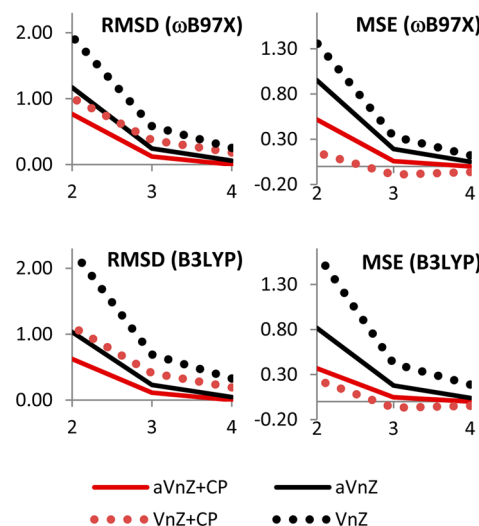


Figure 9. RMSD (Root Mean Square Deviation) and MSE (Mean Signed Deviation) in kcal/mol for the (a)VnZ basis sets ($n = 2, 3, 4$), including or not the counterpoise (CP) correction, for the ω B97X and B3LYP functionals. The reference (an almost “complete basis set”) was aVQZ+CP.

Other basis sets were tested with the ω B97X and B3LYP (see Table 7) functionals, taking as reference energies the aVQZ+CP level (considered as a virtually complete basis set in DFT). Not surprisingly, the small double- ζ basis sets (Def2-SVP, SDD, and LANL2DZ) are quite terrible, strongly overbinding as usual when having basis set superposition error. Def2-SVP is more accurate than the others, but that is expected as it is the only one with polarization functions between the analyzed double- ζ . The bigger basis sets show a significant improvement. However, going from Def2-TZVP to Def2-QZVP or even to the augmented one does not increase the accuracy significantly. On a closer look at the bromine or iodine systems, we can see that the I ones are well described by the QZVP, but the Br systems are not converging to the reference values. This error can be tracked to the fact that the Def2 basis set for Br is not an ECP, thus lacking the relativistic effects. The error in the bromine systems is actually close to the error seen in Table 6, when we compared relativistic to nonrelativistic DFT.

We can conclude that for practical purposes the use of a good augmented triple- ζ would be the right choice, but aVQZ or aVTZ+CP (the “PP” version of them, with an ECP) should be used if higher accuracy is desired.

Assessment of Wave Function Methods. As can be seen in Figure 10 and Table 8, wave function methods tend to be more accurate than DFT (see also Figure 11), but of course at the expense of more computational time (with the obvious exception of the useless Hartree–Fock). The accuracy grows approximately with the complexity of the method, with HF < MP2 < CCSD < CEPA1 < CCSD(T). However, similar to the geometry results of the XB18 set (Tables 3 and 4), spin component-scaling the MP2 correlation strongly improves the results. Again, it is not important to scale down the same spin correlation (as in SCS-MP2) or the opposite spin one (as in SCS(MI)MP2), as long as the total MP2 correlation is lowered.

The recommended basis set is, again, at least aVTZ. MP2 overbinds (positive MSE); thus, as a consequence of the BSSE, a small basis set degrades the accuracy even more. The exception is the underbinding SCS-MP2, consistent with a

Table 7. RMSD and MSE for Different Basis Sets with ω B97X and B3LYP, Taking As Reference Energies the Same Functionals at the aVQZ+CP Basis Set^a

		XB51		Br		I	
		MSE	RMSD	MSE	RMSD	MSE	RMSD
ω B97X	aug-Def2-QZVP	-0.14	0.31	-0.39	0.50	0.00	0.03
	Def2-QZVP	-0.16	0.35	-0.44	0.55	-0.01	0.09
	Def2-TZVP	0.06	0.47	-0.15	0.54	0.16	0.42
	Def2-SVP	1.38	1.98	1.26	1.77	1.45	2.11
	SDD	2.55	3.67	3.11	4.14	2.07	3.20
	LANL2DZ	2.13	3.36	2.73	3.84	1.61	2.88
B3LYP	aug-Def2-QZVP	-0.13	0.30	-0.38	0.48	0.01	0.04
	Def2-QZVP	-0.12	0.32	-0.39	0.50	0.02	0.12
	Def2-TZVP	0.12	0.51	-0.05	0.55	0.20	0.47
	Def2-SVP	1.55	2.24	1.38	2.04	1.67	2.40
	SDD	3.02	3.99	3.62	4.47	2.54	3.56
	LANL2DZ	2.41	3.47	2.92	3.78	1.96	3.10

^aThe “Br” and “I” columns correspond to the XB51 systems based on those elements.

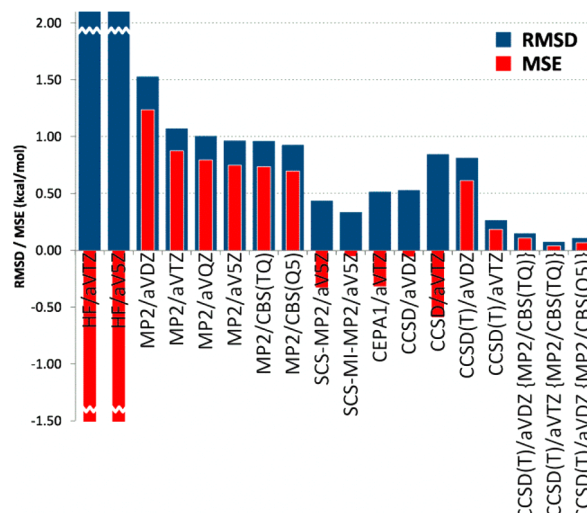


Figure 10. Root mean square deviation and mean signed error for wave function methods in kcal/mol, for the dissociation energy of the XB51 set (reference energies: $E_{\text{CBS}/\text{MP2}(\text{QS})}^{\text{CCSD(T)}/\text{vVTZ}}$, see eq 2). All the MP2 calculations include the density fitting approximation. The last three columns are CBS extrapolations according to eq 2.

small same spin correlation (the “long range” one); in this particular case using a small basis set will not be so deleterious. The same happens with CCSD, which has a better performance with aVDZ compared to aVTZ, thanks to error compensation. At the CCSD(T) level, aVDZ is not a sensible option. However, if it is extrapolated to a complete basis set with MP2 (eq 2), then the accuracy beats the much more expensive CCSD(T)/aVTZ (especially when including the density fitting approximation on the MP2 part). Within the CBS extrapolation, using aVQZ/aVSZ basis sets for the MP2 part brings only a small improvement over the faster aVTZ/aVQZ.

In summary, for systems where CCSD(T)/aVQZ is unfeasible, two wave function methods are a good compromise: CBS extrapolation ($E_{CBS/MP2(TQ)}^{CCSD(T)/aVDZ}$, eq 2) and SCS-MP2 (or SCS(MI)MP2), both with density fitting if possible.

Assessment of DFT Methods. As halogen bonds are a combination of different bonding models (dispersion, electrostatics, charge transfer, etc.), DFT has a hard time covering all the bases for their proper description. On average, there is an improvement when climbing Jacob's ladder,⁸² but with a large

Table 8. Root Mean Square Deviation, Mean Signed Error, and Maximum Error for Wave Function Methods in kcal/mol, for the Dissociation Energy of the XB51 Set^a

	RMSD	MSE	max. error
HF/aVTZ	4.62	-3.92	-12.72
HF/aVSZ	4.81	-4.09	-13.10
MP2/aVDZ	1.53	1.24	5.12
MP2/aVTZ	1.07	0.88	3.18
MP2/aVQZ	1.00	0.80	2.86
MP2/aVSZ	0.96	0.75	2.70
MP2/CBS(TQ)	0.96	0.74	2.62
MP2/CBS(Q5)	0.92	0.70	2.54
SCS-MP2/aVSZ	0.44	-0.33	-1.41
SCS-MI-MP2/aVSZ	0.33	-0.05	0.84
CEPA1/aVTZ	0.51	-0.32	-1.47
CCSD/aVDZ	0.53	-0.06	-1.65
CCSD/aVTZ	0.85	-0.59	-2.71
CCSD(T)/aVDZ	0.81	0.61	2.64
CCSD(T)/aVTZ	0.26	0.19	0.67
$E_{\text{CBS}/\text{MP2}(\text{TQ})}^{\text{CCSD(T)}/\text{aVDZ}}$	0.15	0.11	0.42
$E_{\text{CBS}/\text{MP2}(\text{TQ})}^{\text{CCSD(T)}/\text{aVTZ}}$	0.07	0.04	0.21
$E_{\text{CBS}/\text{MP2}(\text{Q5})}^{\text{CCSD(T)}/\text{aVDZ}}$	0.11	0.07	0.34
$E_{\text{CBS}/\text{MP2}(\text{Q5})}^{\text{CCSD(T)}/\text{aVTZ}}$	0	by def.	

^aAll the MP2 calculations include the density fitting approximation.

variability of values for each rung (see Figure 11 and Table 9). GGA-DFT cannot be recommended, except for the M06L functional, and to a lesser degree B97D. Between the hybrid functionals, M06-2X is a clear leader, showcasing the capabilities of the Minnesota family of functionals.^{88,92} The improvement over its M06 sibling makes us wonder if high exact exchange is an important factor for these bonds, a matter that we will discuss below. Long-range corrected hybrids, with a variable amount of exact exchange, are all over the map. However, ω B97XD⁹³ is almost as accurate as M06-2X, indicating that halogen bonds require a subtle equilibrium between exact and DFT exchange. Double hybrids^{84,94,95} match the accuracy of SCS-MP2 and M06-2X and are consistently better than lower rungs on Jacob's ladder. Their uniform accuracy all along the periodic table makes them a suitable method when the system under study includes more than halogen bonds. DSD-PBEh-B95 and DSD-PBE-P86 are the winners by a hairbreadth.^{84,96}

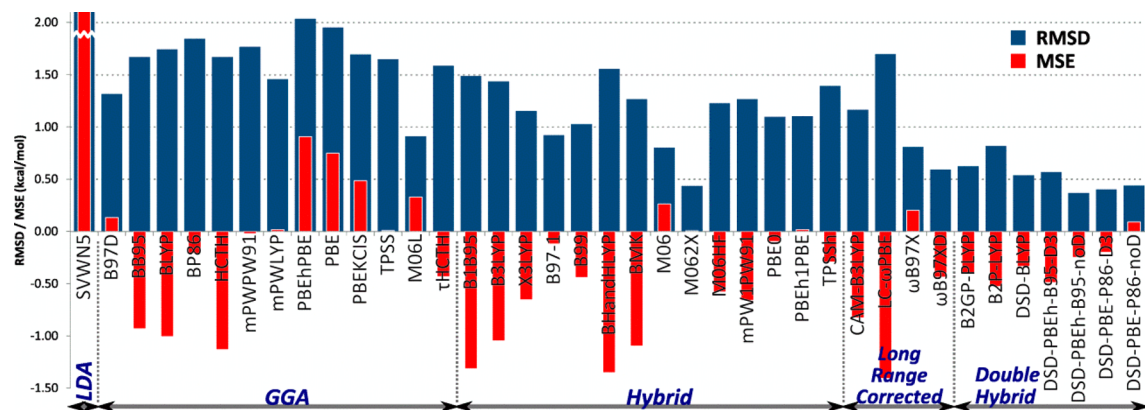


Figure 11. Root mean square deviation and mean signed error for DFT methods in kcal/mol, for the dissociation energy of the XB51 set, with aVTZ+CP basis set (reference energies: $E_{\text{CBS/MP2(QS)}}^{\text{CCSD(T)/aVTZ}}$, see eq 2).

Table 9. Root Mean Square Deviation, Mean Signed Error, and Maximum Error for DFT Methods in kcal/mol, for the Dissociation Energy of the XB51 Set, with aVTZ+CP Basis Set (Reference Energies: $E_{\text{CBS/MP2(QS)}}^{\text{CCSD(T)/aVTZ}}$, see eq 2)

		RMSD	MSE	max. error
LDA	SVWN5	5.58	4.42	12.54
GGA	B97D	1.31	0.13	5.56
	BB95	1.67	-0.93	3.65
	BLYP	1.74	-1.01	-5.01
	BP86	1.84	-0.21	6.05
	HCTH	1.67	-1.13	-4.59
	mPWPW91	1.77	-0.02	5.97
	mPW-LYP	1.45	0.02	4.93
	PBEhPBE	2.04	0.91	6.68
	PBE	1.95	0.75	6.58
	PBEKCIS	1.69	0.49	6.58
	TPSS	1.65	0.01	4.66
	M06L	0.91	0.33	2.84
	tHCTH	1.59	-0.43	5.28
hybrid	B1B95	1.49	-1.31	-3.13
	B3LYP	1.43	-1.05	-4.36
	X3LYP	1.15	-0.65	-3.81
	b971	0.92	-0.12	2.89
	B98	1.02	-0.44	-2.95
	BHandHLYP	1.55	-1.35	-4.01
	BMK	1.27	-1.10	-2.81
	M06	0.80	0.27	1.97
	M062X	0.43	0.01	1.58
	M06HF	1.22	-0.58	3.62
	mPW1PW91	1.27	-0.66	-3.35
	PBE0	1.10	-0.10	2.91
	PBEh1PBE	1.10	0.02	2.96
	TPSSh	1.39	-0.29	3.41
long range corrected	CAM-B3LYP	1.16	-0.83	-3.50
	LC-wPBE	1.70	-1.41	-6.20
	wB97X	0.81	0.20	-4.03
	wB97XD	0.59	-0.44	-2.02
double hybrid	B2GP-PLYP	0.62	-0.40	-2.03
	B2PLYP	0.82	-0.53	-2.57
	DSD-BLYP	0.54	-0.33	-1.73
	DSD-PBEh-B95-D3	0.57	-0.49	-1.30
	DSD-PBEh-B95-noD	0.37	-0.25	-0.82
	DSD-PBE-P86-D3	0.40	-0.20	-1.28
	DSD-PBE-P86-noD	0.44	0.09	1.19

It must be noted that in a previous study, Lu et al. found that PBE-KCIS, mPW-LYP, and B97-1 gave the best performance for the systems and methods they surveyed.³¹ We included these functionals in our evaluation pool, and although the first two were found to be of dubious quality, B97-1 was indeed among the best ones.

In summary, depending on the size of the system, we can recommend for halogen bonds the following functionals, ordered according to their accuracy and computational expense: M06L < ω B97XD < M06-2X < DSD-PBE-P86 (or DSD-PBEh-B95).

Dispersion Correction. Traditional DFT lacks long-range dispersion forces; thus a series of corrections has been devised to tackle this problem. Among the most simple and yet useful, the dispersion corrections of Grimme^{98,99} have been very popular lately. These include the original “D2” method (which calculates a pairwise r^{-6} potential between all the atoms) and the two versions of “D3” (which vary the potentials according to the environment of the atoms and add an r^{-8} term), “D3Zero” (with a damping function that goes to zero) and “D3BJ” (damping going to a finite value).⁹⁷

We have tested the effect of adding these corrections to four functionals (see Figure 12). Being a long-range interaction, the dispersion corrections may be expected to improve the DFT accuracy of halogen bonds. However, as said before, XB is a complex mixture of several types of interactions, and it has been argued that some functionals may compensate the lack of dispersion with an overestimation of the charge transfer⁴⁸ (akin to hydrogen bonds⁷). Therefore, it is possible that a functional

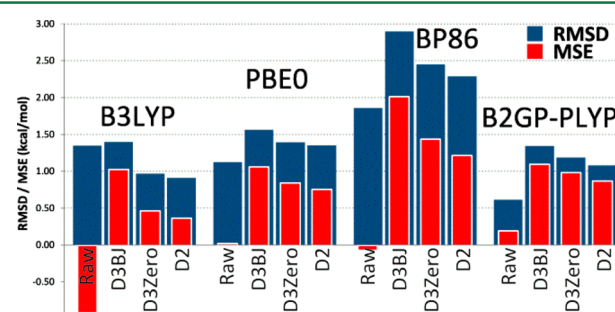


Figure 12. Root mean square deviation and mean signed error for four DFT functionals with and without dispersion corrections (in three different flavors, D2, D3Zero, and D3BJ^{97,98}) in kcal/mol, for the dissociation energy of the XB51 set.

that correctly describes charge transfer will be improved by the addition of a dispersion correction. This is difficult to test, but a comparison of the long-range corrected functionals ω B97X and ω B97XD, which provide a good performance on charge transfer reactions, shows a small improvement in the version that includes the dispersion correction.

We have observed this compensating trend in the XB51 set. For the PBE0, BP86, and B2GP-PLYP functionals, the addition of dispersion corrections degrades accuracy, overbinding the systems that previously had a negligible bias (almost zero MSE). The only functional that is improved is B3LYP, which is known for severely underestimating dispersion forces. And even in this case, the “D3BJ” method brings more problems than solutions (despite the fact that it is considered the more “physically correct” version of Grimme’s methods⁹⁷).

In summary, halogen bonds are just too complex for simple dispersion corrections. Unless based on specific benchmark studies, it is better not to include them in XB systems. For specific circumstances where the molecules may have important van der Waals interactions, then we can recommend the M06 family of functionals, which intrinsically cover dispersion and work well with XB.

Exact-Exchange in Hybrid DFT. We saw before (Figure 11) that even though all the M06-based functionals provide good accuracy for the halogen bonds, M06-2X is by far the best of the family. The high amount of exact (“HF”) exchange in it made us wonder if that is the factor that made this functional so accurate. Therefore, we tested four functionals according to the amount of HF, and the results speak by themselves (see Figure 13).

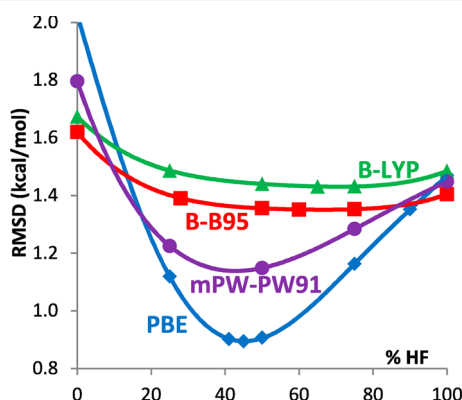


Figure 13. Effect of the percentage of exact exchange on the RMSD (in kcal/mol) over the XB51 set for four functionals.

DFT with B88 exchange (B-LYP and B-B95 in the graph) has a rather flat surface, but the highest accuracy is between 30% and 90% exact exchange. With mPW and PBE exchange, there is a sharp minimum around 40% to 50% HF, a sign that halogen bonds are comfortable with very high exact exchange. Considering that M06-2X has a very high 54% HF, its accuracy is not unexpected. Still, too much exact exchange is detrimental, as can be witnessed from Figure 13 and by the inaccurate M06-HF, which has 100% HF (see Figure 11 and Table 9).

The charge transfer (CT) aspect of the XB may be responsible for the high amount of exact exchange needed. A graph of Hirshfeld charges vs the dissociation energy of all the NH₃ based systems shows that the stronger the halogen bond, the higher the amount of negative charge shifted to the halogen donor (see Supporting Information), showing the CT character

of these dimers. CT is very sensible to self-interaction error,¹⁰⁰ to integer discontinuities of the donor and acceptor molecules,¹⁰¹ and to a good estimation of the HOMO–LUMO gap¹⁰² (there is a natural connection between accurate excitation energies and CT¹⁰⁰). Most DFT functionals cannot model the 1/R asymptotic behavior required by CT systems,^{100,103} unless the HF term is boosted up to approximately 50%.¹⁰² It is worth noting that the more famous sibling of XB, the H-bonds, also suffers from the same malady¹⁰⁴ (actually, both types of bonding are based on the same type of interactions¹⁰⁵).

It has been argued by Steinmann et al. that the accuracy of M06-2X can be attributed to the good treatment of dispersion forces at medium range, more than to the high HF weight.⁴⁸ However, the other functionals of this family tested here (M06-L, M06, and M06-HF) also consider dispersion forces, and even though they are good methods for XB, M06-2X doubles their accuracy. This can only be explained by the higher HF term.

Similarly, some long-range corrected functionals (especially ω B97XD, see Figure 11) were found to be capable of describing the difficult halogen bond. The parametrization of these functionals usually considers excitation energies and TD-DFT calculations,^{106,107} and as we mentioned before, correct excitations will provide accurate charge transfer. By their construction, long-range corrected functionals have high HF at long distances, helping the CT without affecting short-range interactions,¹⁰⁸ which are well described by pure DFT.

CONCLUSIONS

In this “tour,” we started looking at some chemical tools that help analyze the halogen bond (XB), especially the NCI method^{45,66,67} that pinpoints the position and extent of noncovalent bonds and the NOFF⁷⁶ that shows the natural orbitals involved in the charge transfer of the XB.

The second “waystation” was the generation of two benchmarks for XB. The smaller one, XB18, was used to test the behavior of several DFT and wave function methods on their geometries. The bigger one, XB51, which covers a wider range of chemical systems and energies, was designed to test the methods on dissociation energies of the dimers. From this, we can conclude that:

- Halogen bonds are not easy to calculate with high accuracy, due to the mixture of bonding “unicorns.”⁵⁰ A proficient theoretical method must deal with electrostatic, dispersion, polarization, and charge transfer in an efficient way.

- There is, to some extent, a correlation between methods that provide good geometries and good energies. However, this is not a fixed rule. For instance, double hybrids are consistently very accurate on energies, but in the geometry optimizations some hybrid functionals gave better results.

- MP2 cannot be recommended, as it strongly overbinds. Scaling down the correlation by approximately 20% dramatically improves it. Interestingly, it does not matter if the scaled part is the same spin contribution (associated with long-range interactions) or the opposite spin one (for short-range interactions), and therefore SCS-MP2 and SCS(MI)MP2 have similar accuracy, even though they were parametrized for radically different bonding situations.

- The heavier wave function methods have dissimilar performance. MP3, SCS-MP3, and CCSD are not advisable, but MP2.5, SCS-CCSD, and SCS(MI)CCSD are close to CCSD(T) accuracy.

• Complete basis set extrapolation techniques work well with CCSD(T) in XB. Even CCSD(T)/aVDZ with DF-MP2 basis set extrapolation at the aVTZ/aVQZ level gives very accurate and robust results, at a modest computational time (for an ab initio method).

• A large basis set is a must. At least a good triple- ζ with diffuse functions is required. For high accuracy, we must grow to a quadruple- ζ or/and including counterpoise correction. Relativistic ECP is also important, even for the relatively small Br atom.

• A high amount of exact exchange is necessary for good geometries and energies within DFT. The only GGA with respectable accuracy is M06-L. For large systems where the computational time may be an issue, this is a good option (especially considering the wider availability of density fitting techniques on pure GGAs).

• For hybrid DFT, M06-2X followed by ω B97XD provides excellent geometries and energies. Both of them have high HF percentage (the second as a long-range corrected functional), which helps mitigate the self-interaction error and the difficult excitation energies required for charge transfer reactions.

• Dispersion corrections usually degrade accuracy, over-binding when raw DFT generally does not have a big bias (presumably owing to error cancelation).

• Double hybrids, especially DSD-PBEh-B95 and DSD-PBE-P86, match the accuracy of any simple hybrid functional or MP2 based method, with the advantage of being a robust method for almost any other type of chemical bond, including transition metals.⁸⁴ As a drawback, it is slower than a hybrid functional, and the geometries were surpassed by other methods.

■ ASSOCIATED CONTENT

Supporting Information

XYZ geometries, detailed reaction energies, XB distances, and Hirshfeld charges. This material is available free of charge via the Internet at <http://pubs.acs.org>.

■ AUTHOR INFORMATION

Corresponding Author

*E-mail: kozuchs@mail.com.

Present Address

[§]Center for Advanced Scientific Computing and Modeling (CASCAM), Department of Chemistry, University of North Texas, Denton, TX 76203, United States

Notes

The authors declare no competing financial interest.

■ ACKNOWLEDGMENTS

S.K. was supported by a Koshland Fellowship from the Weizmann Institute. During the course of the research, J.M.L.M. was on leave of absence as the Thatcher Professor of Chemistry at the Weizmann Institute of Science. This research was supported in part by the Weizmann AERI (Alternative Energy Research Initiative) and by a startup grant from the University of North Texas. The authors would like to thank Prof. Milko E. van der Boom for introducing us to this topic and Dr. Jean-François Lamère for preliminary calculations.

■ REFERENCES

- (1) Metrangolo, P.; Resnati, G.; Desiraju, G. R.; Ho, P. S.; Kloo, L.; Legon, A. C.; Marquardt, R.; Politzer, P.; Rissanen, K. "Project: Categorizing Halogen Bonding and Other Noncovalent Interactions Involving Halogen Atoms. <http://www.halogenbonding.eu/>" (accessed on February, 2013).
- (2) Metrangolo, P.; Neukirch, H.; Pilati, T.; Resnati, G. *Acc. Chem. Res.* **2005**, *38*, 386–395.
- (3) Politzer, P.; Lane, P.; Concha, M.; Ma, Y.; Murray, J. *J. Mol. Model.* **2007**, *13*, 305–311.
- (4) Legon, A. C. *Phys. Chem. Chem. Phys.* **2010**, *12*, 7736–7747.
- (5) Politzer, P.; Murray, J. S. *ChemPhysChem* **2013**, *14*, 278–294.
- (6) Beale, T. M.; Chudzinski, M. G.; Sarwar, M. G.; Taylor, M. S. *Chem. Soc. Rev.* **2013**, *42*, 1667–1680.
- (7) Hobza, P.; Müller-Dethlefs, K. *Non-Covalent Interactions Theory and Experiment*; Royal Society of Chemistry: Cambridge, U. K., 2010; pp 145–153.
- (8) Auffinger, P.; Hays, F. A.; Westhof, E.; Ho, P. S. *Proc. Natl. Acad. Sci. U. S. A.* **2004**, *101*, 16789–16794.
- (9) Hardegger, L. A.; Kuhn, B.; Spinnler, B.; Anselm, L.; Ecabert, R.; Stihle, M.; Gsell, B.; Thoma, R.; Diez, J.; Benz, J.; Plancher, J.-M.; Hartmann, G.; Banner, D. W.; Haap, W.; Diederich, F. *Angew. Chem., Int. Ed.* **2011**, *50*, 314–318.
- (10) Metrangolo, P.; Resnati, G. *Chem.—Eur. J.* **2001**, *7*, 2511–2519.
- (11) Meyer, F.; Dubois, P. *CrystEngComm* **2013**, [Advanced Article] DOI: 10.1039/c2ce26150b.
- (12) Walter, S. M.; Kniep, F.; Rout, L.; Schmidchen, F. P.; Herdtweck, E.; Huber, S. M. *J. Am. Chem. Soc.* **2012**, *134*, 8507–8512.
- (13) Lu, Y.; Li, H.; Zhu, X.; Zhu, W.; Liu, H. *J. Phys. Chem. A* **2011**, *115*, 4467–4475.
- (14) Li, Q.-Z.; Jing, B.; Li, R.; Liu, Z.-B.; Li, W.-Z.; Luan, F.; Cheng, J.-B.; Gong, B.-A.; Sun, J.-Z. *Phys. Chem. Chem. Phys.* **2011**, *13*, 2266–2271.
- (15) Lu, Y.; Li, H.; Zhu, X.; Liu, H.; Zhu, W. *Int. J. Quantum Chem.* **2012**, *112*, 1421–1430.
- (16) Bruckmann, A.; Pena, M.; Bolm, C. *Synlett* **2008**, *2008*, 900–902.
- (17) You, L.-Y.; Chen, S.-G.; Zhao, X.; Liu, Y.; Lan, W.-X.; Zhang, Y.; Lu, H.-J.; Cao, C.-Y.; Li, Z.-T. *Angew. Chem., Int. Ed.* **2012**, *51*, 1657–1661.
- (18) Kniep, F.; Walter, S. M.; Herdtweck, E.; Huber, S. M. *Chem.—Eur. J.* **2012**, *18*, 1306–1310.
- (19) Walter, S. M.; Kniep, F.; Herdtweck, E.; Huber, S. M. *Angew. Chem., Int. Ed.* **2011**, *50*, 7187–7191.
- (20) Dordonne, S.; Crousse, B.; Bonnet-Delpon, D.; Legros, J. *Chem. Commun.* **2011**, *47*, 5855–5857.
- (21) Dimitrijević, E.; Kvak, O.; Taylor, M. S. *Chem. Commun.* **2010**, *46*, 9025–9027.
- (22) Lefevre, G.; Franc, G.; Adamo, C.; Jutand, A.; Ciofini, I. *Organometallics* **2012**, *31*, 914–920.
- (23) Zhang, Y. *J. Mol. Struct.: THEOCHEM* **2010**, *961*, 6–8.
- (24) Sarwar, M. G.; Dragišić, B.; Dimitrijević, E.; Taylor, M. S. *Chem.—Eur. J.* **2013**, *19*, 2050–2058.
- (25) Clark, T.; Hennemann, M.; Murray, J.; Politzer, P. *J. Mol. Model.* **2007**, *13*, 291–296.
- (26) Politzer, P.; Murray, J. S.; Clark, T. *Phys. Chem. Chem. Phys.* **2010**, *12*, 7748.
- (27) Eskandari, K.; Zariny, H. *Chem. Phys. Lett.* **2010**, *492*, 9–13.
- (28) Shields, Z. P.; Murray, J. S.; Politzer, P. *Int. J. Quantum Chem.* **2010**, *110*, 2823–2832.
- (29) Clark, T. *WIREs Comput. Mol. Sci.* **2013**, *3*, 13–20.
- (30) Metrangolo, P.; Murray, J. S.; Pilati, T.; Politzer, P.; Resnati, G.; Terraneo, G. *CrystEngComm* **2011**, *13*, 6593–6596.
- (31) Lu, Y.; Zou, J.; Fan, J.; Zhao, W.; Jiang, Y.; Yu, Q. *J. Comput. Chem.* **2009**, *30*, 725–732.
- (32) Chopra, D.; Row, T. N. G. *CrystEngComm* **2011**, *13*, 2175–2186.
- (33) Bauzá, A.; Quiñonero, D.; Frontera, A.; Deyà, P. M. *Phys. Chem. Chem. Phys.* **2011**, *13*, 20371–20379.

- (34) Huber, S. M.; Jimenez-Izal, E.; Ugalde, J. M.; Infante, I. *Chem. Commun.* **2012**, *48*, 7708–7710.
- (35) Scheiner, S. *Int. J. Quantum Chem.* **2013**, *46*, 280–288.
- (36) Bleiholder, C.; Werz, D. B.; Köppel, H.; Gleiter, R. *J. Am. Chem. Soc.* **2006**, *128*, 2666–2674.
- (37) Cozzolino, A. F.; Vargas-Baca, I.; Mansour, S.; Mahmoudkhani, A. H. *J. Am. Chem. Soc.* **2005**, *127*, 3184–3190.
- (38) Iwaoka, M.; Komatsu, H.; Katsuda, T.; Tomoda, S. *J. Am. Chem. Soc.* **2002**, *124*, 1902–1909.
- (39) Riley, K. E.; Hobza, P. *J. Chem. Theory Comput.* **2008**, *4*, 232–242.
- (40) Jabłoński, M.; Palusiak, M. *J. Phys. Chem. A* **2012**, *116*, 2322–2332.
- (41) Lommerse, J. P. M.; Stone, A. J.; Taylor, R.; Allen, F. H. *J. Am. Chem. Soc.* **1996**, *118*, 3108–3116.
- (42) Palusiak, M. *J. Mol. Struct.* **2010**, *945*, 89–92.
- (43) Wolters, L. P.; Bickelhaupt, F. M. *ChemistryOpen* **2012**, *1*, 96–105.
- (44) Tsuzuki, S.; Wakisaka, A.; Ono, T.; Sonoda, T. *Chem.—Eur. J.* **2012**, *18*, 951–960.
- (45) Pinter, B.; Nagels, N.; Herrebout, W. A.; De Proft, F. *Chem.—Eur. J.* **2013**, *19*, 519–530.
- (46) Wang, W.; Hobza, P. *J. Phys. Chem. A* **2008**, *112*, 4114–4119.
- (47) Noumenon (plural noumena): In the philosophy of Immanuel Kant... a thing as it is independent of any conceptualization or perception by the human mind; a thing-in-itself, postulated by practical reason but existing in a condition which is in principle unknowable and unexperienceable. (From Wiktionary, <http://en.wiktionary.org>, accessed February 2013).
- (48) Steinmann, S. N.; Piemontesi, C.; Delachat, A.; Corminboeuf, C. *J. Chem. Theory Comput.* **2012**, *8*, 1629–1640.
- (49) Gonthier, J. F.; Steinmann, S. N.; Wodrich, M. D.; Corminboeuf, C. *Chem. Soc. Rev.* **2012**, *41*, 4671.
- (50) Frenking, G.; Krapp, A. *J. Comput. Chem.* **2006**, *28*, 15–24.
- (51) Wikipedia. <http://en.wikipedia.org/wiki/Siren> (accessed February, 2013).
- (52) Jorgensen, W. L.; Schyman, P. *J. Chem. Theory Comput.* **2012**, *8*, 3895–3901.
- (53) Chudzinski, M. G.; Taylor, M. S. *J. Org. Chem.* **2012**, *77*, 3483–3491.
- (54) Řezáč, J.; Riley, K. E.; Hobza, P. *J. Chem. Theory Comput.* **2012**, *8*, 4285–4292.
- (55) Halkier, A.; Koch, H.; Jørgensen, P.; Christiansen, O.; Nielsen, I. M. B.; Helgaker, T. *Theor. Chem. Acc.* **1997**, *97*, 150–157.
- (56) Basis set exchange. <https://bse.pnl.gov/bse/portal> (accessed February, 2013).
- (57) Feller, D. *J. Comput. Chem.* **1996**, *17*, 1571–1586.
- (58) Schuchardt, K. L.; Didier, B. T.; Elsethagen, T.; Sun, L.; Gurumoorthi, V.; Chase, J.; Li, J.; Windus, T. L. *J. Chem. Inf. Model.* **2007**, *47*, 1045–1052.
- (59) Peterson, K. A.; Figgen, D.; Goll, E.; Stoll, H.; Dolg, M. *J. Chem. Phys.* **2003**, *119*, 11113–11123.
- (60) Peterson, K. A.; Shepler, B. C.; Figgen, D.; Stoll, H. *J. Phys. Chem. A* **2006**, *110*, 13877–13883.
- (61) Werner, H. J.; Knowles, P. J.; Knizia, G.; Manby, F. R.; Schütz, M.; Celani, P.; Korona, T.; Lindh, R.; Mitrushenkov, A.; Rauhut, G.; Shamasundar, K. R.; Adler, T. B.; Amos, R. D.; Bernhardsson, A.; Berning, A.; Cooper, D. L.; Deegan, M. J. O.; Dobbyn, A. J.; Eckert, F.; Goll, E.; Hampel, C.; Hesselmann, A.; Hetzer, G.; Hrenar, T.; Jansen, G.; Köpli, C.; Liu, Y.; Lloyd, A. W.; Mata, R. A.; May, A. J.; McNicholas, S. J.; Meyer, W.; Mura, M. E.; Nicklass, A.; O'Neill, D. P.; Palmieri, P.; Pflüger, K.; Pitzer, R.; Reiher, M.; Shiozaki, T.; Stoll, H.; Stone, A. J.; Tarroni, R.; Thorsteinsson, T.; Wang, M.; Wolf, A. *MOLPRO*, version 2010.1; Cardiff University: Cardiff, U. K.; Universität Stuttgart: Stuttgart, Germany, 2010.
- (62) Werner, H.-J.; Knowles, P. J.; Knizia, G.; Manby, F. R.; Schütz, M. *WIREs Comput. Mol. Sci.* **2011**, *2*, 242–253.
- (63) Frisch, M. J.; Trucks, G. W.; Schlegel, H. B.; Scuseria, G. E.; Robb, M. A.; Cheeseman, J. R.; Scalmani, G.; Barone, V.; Mennucci, B.; Petersson, G. A.; Nakatsuji, H.; Caricato, M.; Li, X.; Hratchian, H. P.; Izmaylov, A. F.; Bloino, J.; Zheng, G.; Sonnenberg, J. L.; Hada, M.; Ehara, M.; Toyota, K.; Fukuda, R.; Hasegawa, J.; Ishida, M.; Nakajima, T.; Honda, Y.; Kitao, O.; Nakai, H.; Vreven, T.; Montgomery, J. A., Jr.; Peralta, J. E.; Ogliaro, F.; Bearpark, M.; Heyd, J. J.; Brothers, E.; Kudin, K. N.; Staroverov, V. N.; Kobayashi, R.; Normand, J.; Raghavachari, K.; Rendell, A.; Burant, J. C.; Iyengar, S. S.; Tomasi, J.; Cossi, M.; Rega, N.; Millam, J. M.; Klene, M.; Knox, J. E.; Cross, J. B.; Bakken, V.; Adamo, C.; Jaramillo, J.; Gomperts, R.; Stratmann, R. E.; Yazayev, O.; Austin, A. J.; Cammi, R.; Pomelli, C.; Ochterski, J. W.; Martin, R. L.; Morokuma, K.; Zakrzewski, V. G.; Voth, G. A.; Salvador, P.; Dannenberg, J. J.; Dapprich, S.; Daniels, A. D.; Farkas, Ö.; Foresman, J. B.; Ortiz, J. V.; Cioslowski, J.; Fox, D. J. *Gaussian 09*, revision C.1; Gaussian, Inc.: Wallingford, CT, 2009.
- (64) Grimme, S.; Antony, J.; Ehrlich, S.; Krieg, H. *DFT-D3 - A dispersion correction for DFT-functionals.* <http://toc.uni-muenster.de/DFTD3> (accessed February, 2013).
- (65) NCI Plot. <http://www.chem.duke.edu/~yang/Software/softwareNCI.html> (accessed in February, 2013).
- (66) Johnson, E. R.; Keinan, S.; Mori-Sánchez, P.; Contreras-García, J.; Cohen, A. J.; Yang, W. *J. Am. Chem. Soc.* **2010**, *132*, 6498–6506.
- (67) Contreras-García, J.; Johnson, E. R.; Keinan, S.; Chaudret, R.; Piquemal, J.-P.; Beratan, D. N.; Yang, W. *J. Chem. Theory Comput.* **2011**, *7*, 625–632.
- (68) Humphrey, W.; Dalke, A.; Schulten, K. *J. Mol. Graphics* **1996**, *14*, 33–38.
- (69) Laurence, C.; Graton, J.; Berthelot, M.; El Ghomari, M. *J. Chem.—Eur. J.* **2011**, *17*, 10431–10444.
- (70) Cristiani, F.; Devillanova, F. A.; Garau, A.; Isaia, F.; Lippolis, V.; Verani, G. *Heteroat. Chem.* **1994**, *5*, 421–428.
- (71) Laurence, C.; Ghomari, M. J. E.; Questel, J.-Y. L.; Berthelot, M.; Mokhlisse, R. *J. Chem. Soc., Perkin Trans. 2* **1998**, 1545–1552.
- (72) Zhou, P.-P.; Qiu, W.-Y.; Liu, S.; Jin, N.-Z. *Phys. Chem. Chem. Phys.* **2011**, *13*, 7408–7418.
- (73) Parr, R. G.; Yang, W. *J. Am. Chem. Soc.* **1984**, *106*, 4049–4050.
- (74) Chattaraj, P. K. *Chemical Reactivity Theory: a Density Functional View*; Taylor & Francis: Boca Raton, FL, 2009; pp 255–265.
- (75) Note that the active basic region should be a ring encompassing both p_y and p_x . However, the Fukui function works with the density of the cationic species, which has already lost one electron. This electron must come from one defined p orbital, thus showing two opposing poles where the electrostatic potential depicts a ring.
- (76) Zhou, P.; Ayers, P. W.; Liu, S.; Li, T. *Phys. Chem. Chem. Phys.* **2012**, *14*, 9890.
- (77) Grimme, S. *J. Chem. Phys.* **2003**, *118*, 9095.
- (78) Distasio, R. A.; Head-Gordon, M. *Mol. Phys.* **2007**, *105*, 1073–1083.
- (79) Grimme, S. *J. Comput. Chem.* **2003**, *24*, 1529–1537.
- (80) Takatani, T.; Hohenstein, E. G.; Sherrill, C. D. *J. Chem. Phys.* **2008**, *128*, 124111.
- (81) Pitoňák, M.; Řezáč, J.; Hobza, P. *Phys. Chem. Chem. Phys.* **2010**, *12*, 9611–9614.
- (82) Perdew, J. P.; Schmidt, K. *AIP Conf. Proc.* **2001**, *577*, 1–20.
- (83) Zhao, Y.; Truhlar, D. G. *J. Phys. Chem. A* **2006**, *110*, 13126–13130.
- (84) Kozuch, S.; Martin, J. M. Submitted.
- (85) Yanai, T.; Tew, D. P.; Handy, N. C. *Chem. Phys. Lett.* **2004**, *393*, 51–57.
- (86) Boese, A. D.; Martin, J. M. L. *J. Chem. Phys.* **2004**, *121*, 3405.
- (87) Karton, A.; Tarnopolsky, A.; Lamére, J.-F.; Schatz, G. C.; Martin, J. M. L. *J. Phys. Chem. A* **2008**, *112*, 12868–12886.
- (88) Zhao, Y.; Truhlar, D. G. *Theor. Chem. Acc.* **2007**, *120*, 215–241.
- (89) Wheeler, S. E.; Houk, K. N. *J. Chem. Theory Comput.* **2010**, *6*, 395–404.
- (90) Zordan, F.; Brammer, L.; Sherwood, P. *J. Am. Chem. Soc.* **2005**, *127*, 5979–5989.
- (91) Hobza, P.; Müller-Dethlefs, K. *Non-Covalent Interactions Theory and Experiment*; Royal Society of Chemistry: Cambridge, U. K., 2010; pp 46–63.

- (92) Zhao, Y.; Truhlar, D. G. *Acc. Chem. Res.* **2008**, *41*, 157–167.
- (93) Chai, J.-D.; Head-Gordon, M. *Phys. Chem. Chem. Phys.* **2008**, *10*, 6615–6620.
- (94) Grimme, S. *J. Chem. Phys.* **2006**, *124*, 034108.
- (95) Kozuch, S.; Gruzman, D.; Martin, J. M. L. *J. Phys. Chem. C* **2010**, *114*, 20801–20808.
- (96) Kozuch, S.; Martin, J. M. L. *Phys. Chem. Chem. Phys.* **2011**, *13*, 20104–20107.
- (97) Grimme, S.; Ehrlich, S.; Goerigk, L. *J. Comput. Chem.* **2011**, *32*, 1456–1465.
- (98) Grimme, S. *WIREs Comput. Mol. Sci.* **2011**, *1*, 211–228.
- (99) Grimme, S. *J. Comput. Chem.* **2004**, *25*, 1463–1473.
- (100) Dreuw, A.; Head-Gordon, M. *J. Am. Chem. Soc.* **2004**, *126*, 4007–4016.
- (101) Tozer, D. J. *J. Chem. Phys.* **2003**, *119*, 12697–12699.
- (102) Ruiz, E.; Salahub, D. R.; Vela, A. *J. Am. Chem. Soc.* **1995**, *117*, 1141–1142.
- (103) Adamo, C.; Barone, V. *J. Chem. Phys.* **1998**, *108*, 664–675.
- (104) Pan, P.-R.; Lin, Y.-S.; Tsai, M.-K.; Kuo, J.-L.; Chai, J.-D. *Phys. Chem. Chem. Phys.* **2012**, *14*, 10705.
- (105) Murray, J. S.; Riley, K. E.; Politzer, P.; Clark, T. *Aust. J. Chem.* **2010**, *63*, 1598–1607.
- (106) Tawada, Y.; Tsuneda, T.; Yanagisawa, S.; Yanai, T.; Hirao, K. *J. Chem. Phys.* **2004**, *120*, 8425–8433.
- (107) Tsuneda, T.; Song, J.-W.; Suzuki, S.; Hirao, K. *J. Chem. Phys.* **2010**, *133*, 174101–174101.
- (108) Chai, J.-D.; Head-Gordon, M. *J. Chem. Phys.* **2008**, *128*, 084106–084106.